GEOCHEMISTRY OF THE CENOZOIC VOLCANIC ROCKS OF ROSS ISLAND AND VICINITY, ANTARCTICA

S. S. Goldich
Northern Illinois University

S. B. Treves
University of Nebraska-Lincoln

N. H. Suhr
Pennsylvania State University - Main Campus

J. S. Stuckless
US Geological Survey, Denver, CO

THE JOURNAL OF GEOLOGY

July 1975

GEOCHEMISTRY OF THE CENOZOIC VOLCANIC ROCKS OF ROSS ISLAND AND VICINITY, ANTARCTICA[1]

S. S. GOLDICH, S. B. TREVES, N. H. SUHR, AND J. S. STUCKLESS[2]

Northern Illinois University, DeKalb, Illinois 60115; University of Nebraska, Lincoln, Nebraska 68508; and Pennsylvania State University, University Park, Pennsylvania 16802

ABSTRACT

The Cenozoic volcanic rocks of Ross Island and vicinity, Antarctica, are surface flows, tuffs, breccias, and small intrusives. The prominent rock is basanitoid. Alkali-basalt magma reached the surface over an appreciable length of time and was differentiated to produce a rock series: basanitoid → trachybasalt → phonolite. The alkalic, silica-undersaturated rocks are part of a larger petrologic province composed of volcanic centers in a belt nearly 2,000 km long roughly parallel to the Transantarctic Mountains. Two trends of magmatic differentiation are apparent. At depth the fractional crystallization of olivine, clinopyroxene, and opaque oxide minerals, all of which are abundant as phenocrysts in the basanitoid flows, produced trachybasalt magma. At crustal levels, fractional crystallization of clinopyroxene, apatite, opaque oxides, kaersutite, plagioclase, and anorthoclase developed the phonolitic rocks. Alkali enrichment is marked, and the end-member phonolites contain 11% Na_2O, 5.6% K_2O, and 57% SiO_2. The basanitoids contain relatively large amounts of Ba (~ 400 ppm), Sr ($\sim 1,000$ ppm), and Rb (~ 30 ppm). The concentrations of these and other trace elements in the various rock types support the model of small degrees of partial melting of peridotitic mantle for the derivation of the basanitoid magma, and of magmatic differentiation for the subsequent development of the rock series.

INTRODUCTION

Twenty-nine samples of volcanic rocks from Ross Island and vicinity in Antarctica (fig. 1) were analyzed for major, minor, and trace constituents. This study is part of the Dry Valley Drilling Project (DVDP), a cooperative program sponsored by Japan, New Zealand, and the United States, and was undertaken to obtain information on the exposed volcanic rocks that might be encountered in drilling. The samples were collected by Treves during five field seasons from 1960 to 1971.

Locations are shown on figures 2 and 3, except for sample 5 (fig. 1).

The volcanic rocks of the Ross Island region are part of a larger province that extends for a distance of nearly 2,000 km from Mt. Weaver to the Balleny Islands and is roughly parallel to the Transantarctic Mountains (fig. 1). Hamilton (1972) suggested that the volcanic belt might be called the Ross Sea petrologic province with three major subdivisions: (1) McMurdo, (2) Hallett, and (3) Balleny volcanic provinces. He gave excellent descriptions of the larger features of the major volcanic centers and noted that the McMurdo volcanic province is characterized by high subaerial volcanoes. To the north in the Hallett province, the volcanic rocks are subglacial domes and low subaerial volcanoes.
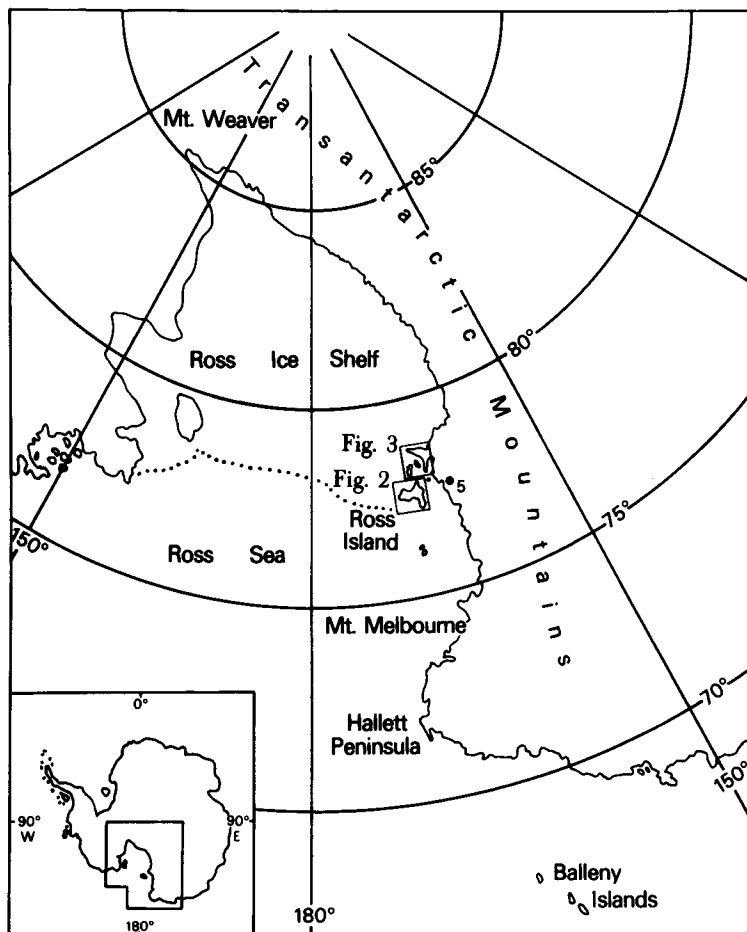
FIG. 1.—Index map of Antarctica showing location of Ross Island area (fig. 2), Mt. Discovery area (fig. 3), and sample no. 5.

The Ross Sea petrologic province is characterized by alkalic, silica-undersaturated Neogene lavas and pyroclastic rocks. The volcanic rocks rest on older rocks of considerable diversity and range in age. These rocks include granite, gneiss, and metasedimentary rocks of late Precambrian and early Paleozoic age, the arenites of the Beacon Supergroup of Devonian to Jurassic age, and diabase sills of the Ferrar Dolerite, dated as Jurassic by McDougall (1963) and Compston et al. (1968).

Outcrops of these old rocks range from sea level to altitudes of 2,000 to 4,000 m

in the Transantarctic Mountains, and xenoliths in the volcanic rocks of the Ross Island vicinity (Prior 1907; Thompson 1916; Forbes 1963) indicate that the Ross Sea region (fig. 1) is underlain by similar rocks. This interpretation is supported by aeromagnetic data (L. D. McGinnis, verbal communication, 1974). The large topographic relief on the western edge of the Ross Sea is interpreted as a zone of normal faulting or sharp flexures (Hamilton 1972).

The rock names used in this paper are based on modal compositions supplemented by chemical and normative data.
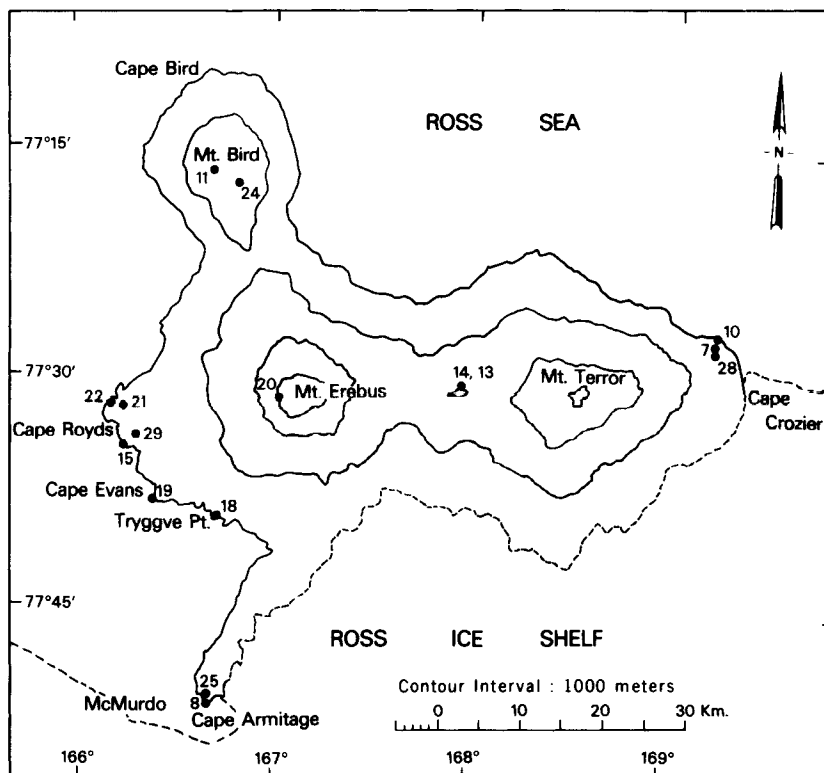
FIG. 2.—Map of Ross Island area showing locations of analyzed samples

At each of the major centers in the Ross Island vicinity there appears to be a succession that ranges from basanitoid to phonolite followed by younger basanitoids (Treves 1967). Pyroclastic deposits of tuff and breccia underlie the lavas as has been confirmed by the core from DVDP drill holes recently completed at McMurdo Station (locality 25, fig. 2).

PRINCIPAL ROCK TYPES

Basanitoid.—Basanitoids are alkalic olivine basalts which contain more than 5% normative nepheline, but no pheno-crystic nepheline (Macdonald and Katsura 1964). With the exception of sample 12, which contains 3.7% of normative nepheline, the range is from 7.6 to 18%, averaging 12% normative nepheline.

Basanitoids occur in nearly every exposure of volcanics in the Ross Island vicinity, and regardless of their relative ages, they are chemically and petro-graphically similar. All display textures from intersertal to granular, with augite, plagioclase, nepheline, and opaques form-ing the groundmass. Olivine and clino-pyroxene are the dominant phenocrysts with most samples containing subhedral to euhedral olivine (Fo_{80}) and titaniferous augite. Less ubiquitous phenocrysts in-clude plagioclase and kaersutite. Labrador-ite phenocrysts occur in only one of the analyzed basanitoids (sample 7) and are not abundant (less than 5%) in other basanitoids in the Ross Island vicinity. They are generally anhedral and resorbed. Kaersutite in three of the analyzed basanitoids is generally subhedral to anhedral and rimmed with, or totally
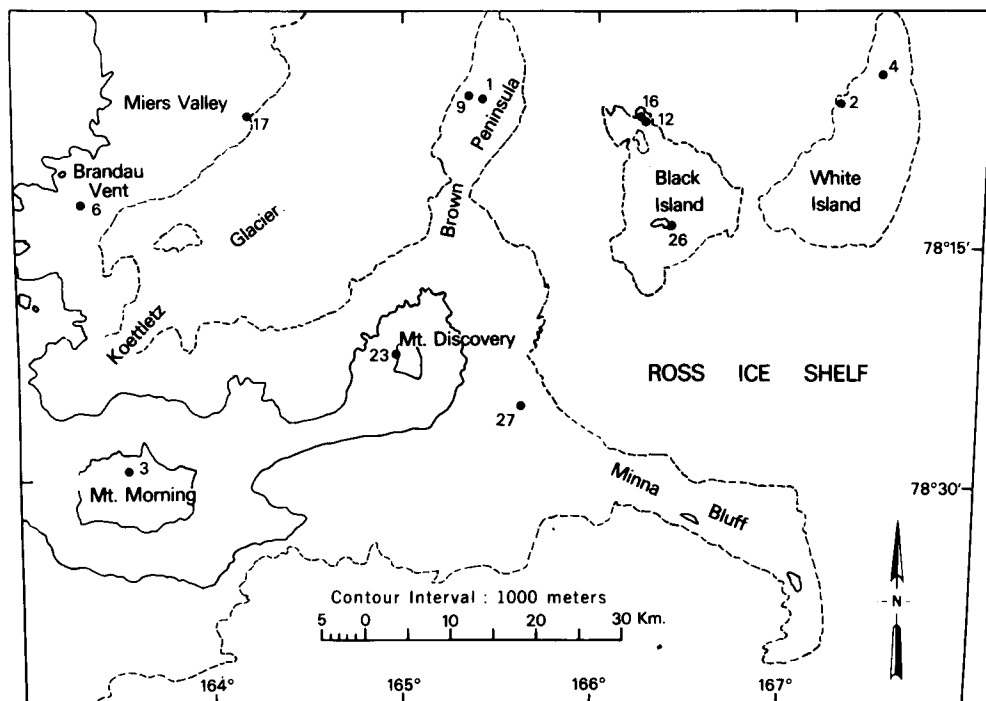
FIG. 3.—Map of Mt. Discovery area showing locations of analyzed samples

replaced by, opaque oxides. Sparse phenocrysts of opaque oxides occur in most of the samples.

Rocks of basanitoid composition occur both as thin flows and pyroclastic cones. The latter often contain ultramafic, mafic, and sedimentary rock inclusions from which small amounts of xenocrystic material, such as labradorite, appear to have been derived.

Trachybasalt.—The trachybasalts are rocks of intermediate composition, between basanitoid and phonolite. These rocks are fairly diverse in chemistry and mineralogy. They are characterized by pilotaxitic to trachytic texture and by plagioclase in the phenocryst assemblages. Like the basanitoids, the trachybasalts are undersaturated with respect to silica. Normative nepheline ranges from 6.3 to 15%, averaging 11%.

Plagioclase, kaersutite, and titaniferous augite are the dominant phenocrysts, each ranging from subhedral to euhedral. Plagioclase, commonly labradorite, makes up 4%–39% of each sample and is normally zoned with a range from An_{65} to An_{35}. Kaersutite in the trachybasalts is not as strongly reacted as that in the basanitoids, but is commonly rimmed by opaque oxides. Accessory phenocrysts include olivine, opaque minerals, and trace amounts of apatite. The groundmass consists of plagioclase, augite, finely disseminated opaques, and, in some samples, a brown glass. At Half Moon Crater, 2 km north of McMurdo Station, a trachybasalt contains abundant mafic and sedimentary rock inclusions.

Anorthoclase phonolite.—Anorthoclase phonolites, or antarctic kenytes (Prior 1907; Smith 1954; Treves 1967), are remarkably uniform in chemistry and mineralogy. Flows crop out on the summit

of Mt. Erebus and on the flanks of the mountain. All are coarsely porphyritic and contain 30%–40% subhedral to euhedral anorthoclase. The texture is trachytic; the groundmass consists of plagioclase, anorthoclase, apatite, opaque minerals, and nepheline. Normative nepheline ranges from 14% to 19% and averages 15%.

Anorthoclase phenocrysts ($Or_{16}Ab_{63}$ An_{21}, Treves 1967) invariably contain inclusions of apatite, glass, augite, opaque materials, and olivine. In one sample with a holocrystalline groundmass, the crystal edges are slightly rounded, and the interior of the crystals exhibits mosaic intergrowths and polysynthetic and cross-hatched twinning. Minor phenocrystic phases include augite, opaque minerals, apatite, and occasional olivine.

The anorthoclase phonolites range in age from at least 0.68 ± 0.14 m.y. (Treves 1967) to present. During the 1972–1973 and 1973–1974 field seasons Mt. Erebus was active, and bombs which were collected on snow and ice at the summit consist of dark-brown glassy, pumiceous anortho-clase phonolite. The upper crater of Mt. Erebus is covered with loose crystals of anorthoclase, many longer than 5 cm which appear to be a lag deposit freed from the pumiceous matrix by weathering.

Mafic phonolites.—The mafic phonolites are quite variable both in amounts and proportions of phenocrysts and in chemistry. Normative nepheline ranges from 13% to 31% and averages 20%. Most samples contain more augite and kaer-sutite than the anorthoclase phonolites, but plagioclase or anorthoclase may be the dominant phenocrysts. Locally, kaersutite is the dominant mafic phenocrysts in younger flows.

Mafic phonolites are ubiquitous in occurrence as small plugs and flows throughout the Ross Island vicinity. They often form prominent topographic features, such as Post Office Hill at Cape Crozier and Observation Hill near Mc-Murdo Station. At most localities, domes intrude and flows overlie basanitoids and locally are partially mantled by younger basanitoids.

Trachyte.—The only analyzed sample which is oversaturated with respect to silica was collected at Mt. Cis between Cape Royds and Cape Evans (fig. 2, no. 29). Although earlier investigations described Mt. Cis as a parasitic cone which contains abundant inclusions (Thompson 1916), it appears to be a pingo which was pushed through the overlying anorthoclase phonolite (Treves 1967). Thompson (1916) and Jensen (1916) described the inclusions in the trachyte as sanidinites, pyroxene granulites, diabase, and metamorphosed sandstone. The abundant inclusions suggest the possibility that the composition of the Mt. Cis rock has been affected by contamination.

ANALYTICAL DATA

Slabs 1 cm thick were cut from the field samples with a diamond saw in water at the University of Nebraska and were used for the preparation of the rock powders at Northern Illinois University. Powder ground to pass an 80-mesh sieve was used for FeO which was determined titrimetrically with $KMnO_4$. Powder ground to pass a 200-mesh sieve was used for all other determinations. Total water was determined by the Penfield method; Na_2O and K_2O by flame photometry; P_2O_5 by colorimetry; SiO_2, Al_2O_3, TiO_2, total Fe, MnO, CaO, MgO, Cu, Zn, and Rb were all determined by atomic absorption spectrophotometry; and the remaining trace elements, by optical spectrography. The methods are essentially those described by Medlin et al. (1970) and Ingamells and Suhr (1963).

Bulk chemical analyses are given in tables 1–4. These include four conventional analyses made at Pennsylvania State University by J. B. Bodkin and J. C. DeVine (see nos. 7, 18, 20, and 21). SiO_2 was determined gravimetrically on 11 of the 29 samples. Other check analyses at

TABLE 1

CHEMICAL ANALYSES OF BASANITOIDS

	1	2	3	4	5	6	7	8	9	10	11	12
SiO$_2$	41.3	42.1	42.5	42.7	43.1	43.3	43.47	43.7	43.8	44.0	44.1	45.0
Al$_2$O$_3$	12.9	13.0	13.3	12.8	14.3	12.8	12.85	11.9	14.5	14.2	14.6	13.3
TiO$_2$	4.08	3.57	3.12	3.27	3.32	3.42	3.28	3.64	3.47	2.83	2.70	3.07
Fe$_2$O$_3$	4.87	3.37	3.00	3.10	4.89	3.19	3.18	1.89	4.56	3.12	3.57	5.30
FeO	7.39	8.90	10.0	7.96	8.55	9.33	9.67	9.04	7.85	7.38	8.77	6.38
MnO	0.20	0.19	0.20	0.19	0.21	0.19	0.19	0.19	0.23	0.19	0.22	0.19
MgO	10.2	11.8	12.1	12.7	8.30	10.9	11.78	12.9	7.75	10.8	8.71	9.50
SrO	0.10	0.11	0.12	0.09	0.12	0.09	0.10	0.10	0.14	0.11	0.11	0.08
CaO	11.0	11.5	10.4	12.5	10.0	12.9	10.60	10.0	10.3	10.5	9.07	12.5
BaO	0.03	0.04	0.04	0.03	0.05	0.03	0.03	0.04	0.07	0.06	0.06	0.03
Na$_2$O	3.59	3.70	2.85	2.85	4.31	2.62	2.93	3.52	4.11	4.38	4.45	2.61
K$_2$O	0.63	0.90	1.17	0.96	1.51	0.93	1.09	1.28	1.78	1.77	1.96	1.03
P$_2$O$_5$	0.82	0.81	0.68	0.63	0.63	0.55	0.58	0.82	0.98	0.65	0.71	0.54
H$_2$O+	1.19	0.45	0.13	0.13	0.20	0.07	0.07	0.19	0.36	0.23	0.15	0.23
H$_2$O-	0.72	0.04	0.03	0.04	0.46	0.03	0.00	0.01	0.07	0.07	0.04	0.30
CO$_2$	0.82	0.02	0.03	0.00	0.02	0.03	0.09	0.01	0.03	0.02	0.03	0.08
Total	99.8	100.5	99.7	100.0	100.0	100.4	99.93*	100.1	100.0	100.2	99.3	100.2

* Total includes F, 0.04; Cl, 0.00; and −0.02 oxygen correction.

TABLE 2

CHEMICAL ANALYSES OF TRACHYBASALTS

	13	14	15	16	17	18
SiO_2	44.5	44.6	45.5	49.5	50.0	50.36
Al_2O_3	16.6	16.9	17.0	17.2	18.7	19.59
TiO_2	3.91	3.46	3.11	2.64	2.36	1.93
Fe_2O_3	6.09	11.8	3.81	2.98	2.85	2.82
FeO	6.01	0.09	8.41	6.38	5.42	5.16
MnO	0.25	0.22	0.24	0.21	0.20	0.20
MgO	4.78	3.78	3.74	2.98	2.58	2.14
SrO	0.15	0.15	0.14	0.12	0.15	0.14
CaO	9.74	9.44	9.30	7.95	6.37	6.46
BaO	0.07	0.07	0.06	0.08	0.07	0.09
Na_2O	4.35	5.37	5.07	5.02	6.35	6.57
K_2O	1.92	2.01	2.13	2.57	3.43	3.32
P_2O_5	1.53	1.39	1.56	1.08	0.99	0.85
H_2O^+	0.20	0.14	0.26	0.73	0.21	0.23
H_2O^-	0.06	0.06	0.10	0.14	0.15	0.03
CO_2	0.03	0.02	0.01	0.02	0.03	0.07
Total	100.2	99.5	100.4	99.6	99.9	100.09*

* Total includes F, 0.14; Cl, 0.06; and −0.07 oxygen correction.

Northern Illinois University included TiO_2 and MnO, colorimetrically; FeO and total Fe, volumetrically; P_2O_5 and H_2O, gravimetrically; and Na_2O and K_2O, photometrically. As a result of these determinations, many of the atomic absorption analyses were repeated. The final analyses represent a combination of methods and have a precision and accuracy approaching that of conventional rock analyses.

The relative errors in the trace-element determinations (tables 5–8) are large compared to the major constituents and are difficult to assess. Rb and Sr were determined by isotope dilution on a composite of basanitoid samples (nos. 1–11) and the results are compared in table 9 with the averages calculated from the values in table 5. The isotope-dilution value for Rb is much less ($\sim 25\%$) and for Sr is greater ($\sim 7\%$) than the averages which represent atomic absorption and emission spectrographic data for Rb and for Sr, respectively. Individual determinations may have larger errors than those indicated by the averages. In contrast with the results for Rb and Sr, determinations of Na_2O and K_2O on the composite

sample (table 9) are in good agreement with the calculated averages.

Major elements.—The samples are very fresh, and with two exceptions the contents of H_2O^+ (above 110°C), H_2O^- (below 110°C), and CO_2 are uniformly low. The exceptions are a basanitoid (table 1, no. 1) from Brown Peninsula (fig. 3) and the trachyte from Mt. Cis (table 4, no. 29; fig. 2).

The basanitoids (table 1) are characterized by SiO_2 contents of less than 45%, high TiO_2, CaO, and MgO, and a range from 0.6% to 2.0% in K_2O. An average of the 12 analyses is given in table 10 (no. 30). The trachybasalts (table 2) are considerably enriched in Na_2O, K_2O, P_2O_5, and Al_2O_3 and are strongly depleted in MgO relative to the basanitoids. The trachybasalts may be further divided into low-silica and high-silica groups (table 10, nos. 31 and 32). TiO_2, P_2O_5, and MnO are markedly enriched in the low-silica trachybasalt relative to the high-silica group.

Four analyses of anorthoclase phonolite (table 3) are similar, and an average is given in table 10 (no. 33). The mafic phonolites (table 4) show a range in

TABLE 3

CHEMICAL ANALYSES OF ANORTHOCLASE PHONOLITES

	19	20	21	22
SiO_2	55.1	55.71	56.10	56.2
Al_2O_3	19.5	18.14	19.57	19.9
TiO_2	1.04	1.22	1.10	1.01
Fe_2O_3	1.91	1.83	1.78	1.91
FeO	4.12	4.90	3.46	3.59
MnO	0.21	0.25	0.19	0.19
MgO	1.13	1.37	1.19	1.16
SrO	0.11	0.10	0.11	0.10
CaO	3.30	3.35	3.24	3.32
BaO	0.12	0.13	0.12	0.12
Na_2O	8.03	7.92	7.80	7.89
K_2O	4.68	4.35	4.26	4.24
P_2O_5	0.42	0.49	0.45	0.46
H_2O^+	0.22	0.11	0.30	0.13
H_2O^-	0.17	0.00	0.14	0.06
CO_2	0.01	0.03	0.07	0.02
F	n.d.	0.15	0.09	n.d.
Cl	n.d.	0.09	0.06	n.d.
Total	100.1	100.14	100.03	100.3
$-O$		0.08	0.05	
Total		100.06	99.98	

TABLE 4

CHEMICAL ANALYSES OF PHONOLITES AND TRACHYTE

	HORNBLENDE AND PYROXENE PHONOLITES						TRACHYTE
	23	24	25	26	27	28	29
SiO_2	54.0	55.0	55.9	56.8	57.3	57.9	58.1
Al_2O_3	19.8	19.6	20.5	21.7	21.6	19.6	15.9
TiO_2	1.42	0.70	0.76	0.27	0.26	0.44	1.00
Fe_2O_3	2.51	3.79	2.65	2.80	1.70	5.16	2.72
FeO	3.83	2.04	1.58	0.64	0.80	0.58	5.06
MnO	0.22	0.12	0.20	0.20	0.17	0.21	0.23
MgO	1.39	1.17	0.87	0.07	0.29	0.44	0.90
SrO	0.17	0.08	0.09	tr	0.05	0.06	0.01
CaO	4.33	3.65	2.98	0.90	1.26	2.17	2.40
BaO	0.16	0.08	0.10	tr	0.07	0.11	0.06
Na_2O	7.18	7.76	9.04	10.95	10.00	8.18	5.28
K_2O	3.85	4.46	4.26	5.56	5.00	4.97	4.98
P_2O_5	0.55	0.23	0.17	0.01	0.03	0.11	0.22
H_2O^+	0.37	0.43	0.35	0.07	0.65	0.01	0.93
H_2O^-	0.22	0.38	0.04	0.13	0.15	0.03	1.26
CO_2	0.03	0.06	0.01	0.01	0.03	0.04	0.06
Total	100.0	99.6	99.5	100.1	99.4	100.0	99.1

TABLE 5

Trace-Element Data for Basanitoids (ppm)

	1	2	3	4	5	6	7	8	9	10	11	12
Ba	290	380	390	300	410	260	280	390	580	510	560	240
Sr	880	960	1,000	740	1,000	760	840	880	1,200	950	950	640
Rb	24	36	33	30	42	36	26	42	49	56	33	36
Cr	460	600	540	870	210	650	760	570	350	430	360	510
Ni	200	170	170	300	110	240	210	290	140	170	170	150
Co	56	56	58	54	54	50	46	49	48	45	44	45
Cu	41	57	37	56	50	64	57	42	32	44	63	85
Zn	110	84	84	120	153	79	112	79	113	78	104	126
Pb	2.4	4.6	1.7	<1	4.5	2.5	2.3	2.5	3.9	5.6	4.8	1.6
Ag	1.4	1.1	1.4	1.2	0.3	0.3	1.7	0.2	1.7	0.2	0.4	0.3
Sn	<3.0	4.2	<3.0	<3.0	3.1	<3.0	<3.0	3.2	4.3	3.1	<3.0	5.1
Be	2.7	3.0	2.2	2.4	2.7	2.2	2.3	3.2	3.5	2.8	3.2	2.2
V	280	290	250	280	240	310	280	260	260	210	190	300
Y	31	35	31	25	31	29	31	21	49	31	24	23
La	52	56	47	43	54	<20	48	59	90	53	70	35
Ce	<100	<100	<100	<100	<100	<100	<100	<100	120	<100	<100	<100
Yb	3.4	3.2	3.5	2.6	3.2	3.6	3.2	2.0	4.8	3.4	2.8	2.7
Zr	330	310	230	240	360	230	290	450	370	330	490	260
K/Rb	218	208	294	266	298	214	354	253	302	262	493	238
Rb/Sr	0.027	0.038	0.033	0.040	0.042	0.047	0.031	0.048	0.041	0.059	0.035	0.056
Ba/Sr	0.33	0.40	0.39	0.41	0.41	0.34	0.33	0.44	0.48	0.54	0.59	0.38

TABLE 6

Trace-Element Data for Trachybasalts (ppm)

	13	14	15	16	17	18
Ba.......................	630	630	510	710	660	760
Sr	1,270	1,270	1,200	1,000	1,270	1,180
Rb	50	60	56	54	72	68
Cr	< 5	< 5	< 5	< 5	< 5	< 5
Ni	14	< 10	< 10	< 10	< 10	< 10
Co	32	26	22	< 10	15	< 10
Cu.....................	34	25	17	36	32	12
Zn	109	111	115	95	91	89
Pb.....................	5.1	3.5	5.0	7.6	4.4	5.2
Ag.....................	0.7	0.3	0.3	0.3	< 0.1	< 0.1
Sn	< 2.5	< 2.5	< 2.5	< 2.5	5.1	3.5
Be.....................	3.5	3.3	3.2	3.1	4.2	4.1
V.......................	190	120	130	130	72	39
Y.......................	37	33	41	37	43	37
La.....................	80	86	80	72	92	94
Ce	< 100	100	110	100	130	130
Yb.....................	3.6	2.9	4.6	3.7	3.6	3.2
Zr	340	410	390	400	490	470
K/Rb	319	278	316	395	395	408
Rb/Sr	0.039	0.047	0.047	0.054	0.057	0.058
Ba/Sr	0.50	0.50	0.43	0.71	0.52	0.64

TABLE 7

Trace-Element Data for Anorthoclase Phonolites (ppm)

	19	20	21	22
Ba	1,070	1,200	1,070	1,070
Sr	930	840	950	900
Rb	97	80	87	91
Cr	< 5	< 5	< 5	< 5
Ni	< 10	13	< 10	< 10
Co...........................	< 10	< 10	< 10	< 10
Cu...........................	39	24	19	20
Zn...........................	118	135	99	98
Pb	5.0	3.3	5.3	6.4
Ag	0.1	0.5	0.4	15
Sn	6.0	3.3	4.2	7.2
Be	6.2	6.2	5.8	6.2
V	< 10	32	16	16
Y............................	61	66	46	55
La	120	140	110	120
Ce	220	240	200	230
Yb	5.0	5.6	4.1	4.9
Zr	640	540	570	590
K/Rb	365	431	379	387
Rb/Sr	0.10	0.095	0.092	0.10
Ba/Sr	1.15	1.43	1.13	1.19

TABLE 8

TRACE-ELEMENT DATA FOR PHONOLITES AND TRACHYTE (ppm)

| | HORNBLENDE AND PYROXENE PHONOLITES | | | | | | TRACHYTE |
	23	24	25	26	27	28	29
Ba	1,430	750	860	~15	580	990	520
Sr	1,440	640	780	<30	420	520	48
Rb	68	112	137	156	173	125	104
Cr	<5	10	10	<5	<5	<5	<5
Ni	<10	12	12	25	<10	<10	<10
Co	<10	<10	<10	<10	<10	<10	<10
Cu	8	30	34	24	19	25	28
Zn	87	124	108	120	98	111	174
Pb	4.9	11	13	15	16	6.6	11
Ag	0.4	<0.1	1.8	7.4	<0.1	0.9	0.1
Sn	<3.0	6.1	<3.0	6.2	3.0	6.5	6.2
Be	4.4	6.1	7.4	8.8	9.4	5.3	6.4
V	16	43	48	<10	<10	<10	<10
Y	46	37	31	43	39	26	74
La	120	130	140	180	120	150	150
Ce	210	260	250	300	200	240-	290
Yb	3.7	3.3	3.2	4.3	3.0	3.1	7.1
Zr	510	960	1,200	620	510	580	620
K/Rb	470	311	258	296	227	330	398
Rb/Sr	0.047	0.18	0.18	...	0.41	0.24	2.1
Ba/Sr	0.99	1.17	1.10	...	1.38	1.90	10.8

TABLE 9

COMPARATIVE DATA CALCULATED FROM INDIVIDUAL ANALYSES AND DETERMINED ON A COMPOSITE OF THE BASANITOID SAMPLES

	Calculated	Determined
Na_2O (wt %) ...	3.57	3.55*
K_2O (wt %) ...	1.27	1.27*
Rb (ppm) ...	37	30†
Sr (ppm) ...	925	993†

* Flame photometry (SSG).
† Isotope dilution (C. E. Hedge).

composition; hence, the average (table 10, no. 34) must be used with caution. These rocks range from 54% to 58% in SiO_2, from 7.0% to 11% in Na_2O, and from 3.8% to 5.6% in K_2O.

The variations of the major constituents with SiO_2 are shown in figure 4. The distribution is bimodal with the gap between 46% and 54% SiO_2 occupied by the high-silica trachybasalts. If the older published analyses from the area are included, a few additional points fall in the

intermediate range. The trends, however, are not altered; the distribution remains bimodal; and the scatter of points is considerably increased as should be expected from chemical analyses made at different times in different laboratories.

Data from published analyses (Prior 1902, 1907; Jensen 1916; Smith 1954; Forbes and Kuno 1965; Boudette and Ford 1966; Cole and Ewart 1968; McIver and Gevers 1970) are included with the new data in figure 5 in which the mole proportions, $CaO:Na_2O:K_2O$, are plotted. The trend is essentially linear with the ratio $Na_2O:K_2O$ nearly constant. The trachyte from Mt. Cis, however, plots well above the trend, and its position is confirmed by an earlier analysis.

The high contents of Na_2O, K_2O, TiO_2, and P_2O_5 characterize the alkali basalts. Of these the behavior of P_2O_5 is difficult to explain. In figure 4 the points for P_2O_5 in the basanitoids form a separate group, a pattern not shown by any other major constituent. In a plot of P_2O_5 against TiO_2
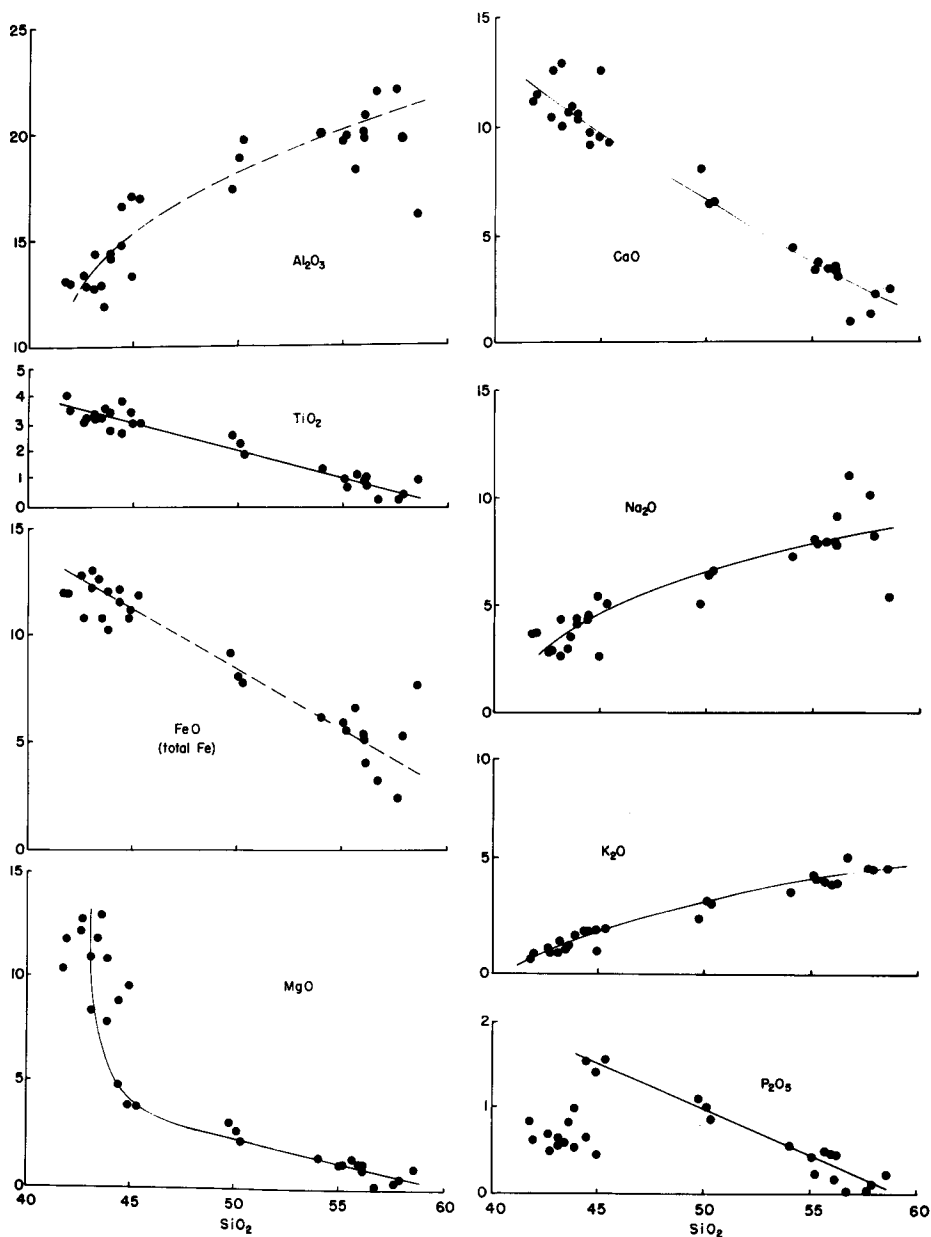
FIG. 4.—Variations of major constituents with SiO_2

(fig. 6), the basanitoid samples again fall in a separate group. Normative apatite ranges from 1.3% to 2.3%, averaging 1.7% in the basanitoids, but in the low-silica trachybasalt the average normative apatite is 3.7%.

Trace elements.—Although the errors in the determinations of the trace elements are large compared to the major constituents, the trends shown in figures 7–10 are real. La and Zr show essentially linear variations with Na (fig. 7). Plots of Yb and
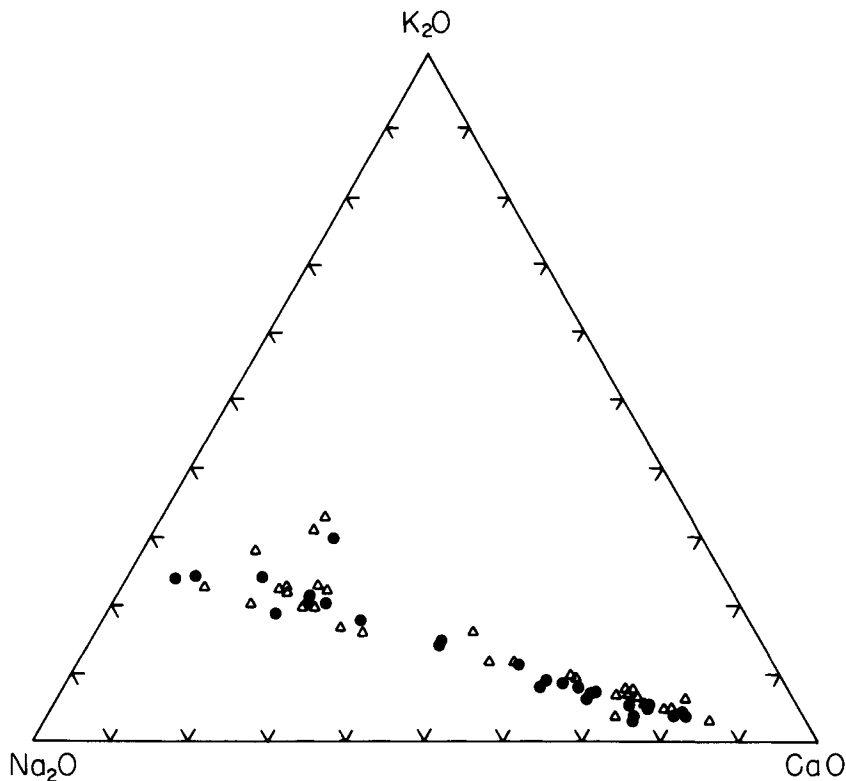
FIG. 5.—$CaO:Na_2O:K_2O$ diagram (mole ratios) for volcanic rocks of Ross Island vicinity. *Filled circles*, new analyses; *triangles*, old analyses from literature.
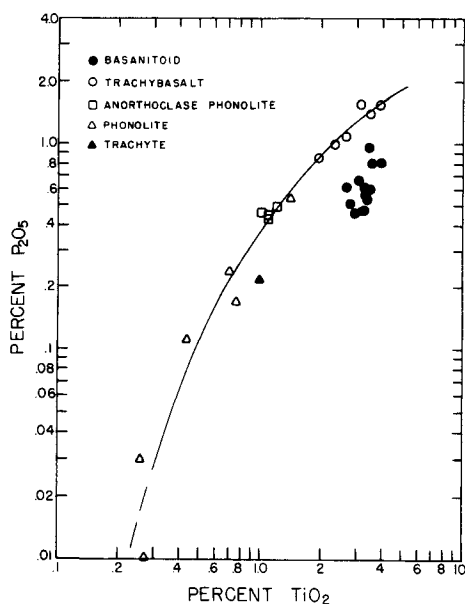
FIG. 6.—Variations of P_2O_5 with TiO_2

Y would show a similar correlation, but the scatter of the points is much greater than for La. In large part, this must be attributed to analytical error. The average La content of the basanitoids is approximately 50 ppm, and La/Yb is about 20. For the mafic phonolites (table 8), the average La content is approximately 140 ppm, and La/Yb is approximately 40. Results from isotope-dilution analyses (Kay and Gast 1973) for similar rock types are of the same order of magnitude.

The variations of Pb and Rb with K (fig. 8) are similar, and the relatively greater scatter in the Pb data is largely analytical error. Rb increases with K content in the basanitoids and trachybasalts, but shows a marked increase in rate of growth in the phonolitic rocks. Like Pb and Rb, Ba and Sr vary with K (fig. 9) along two distinct trends. Both Ba and Sr increase with K content in the basanitoids
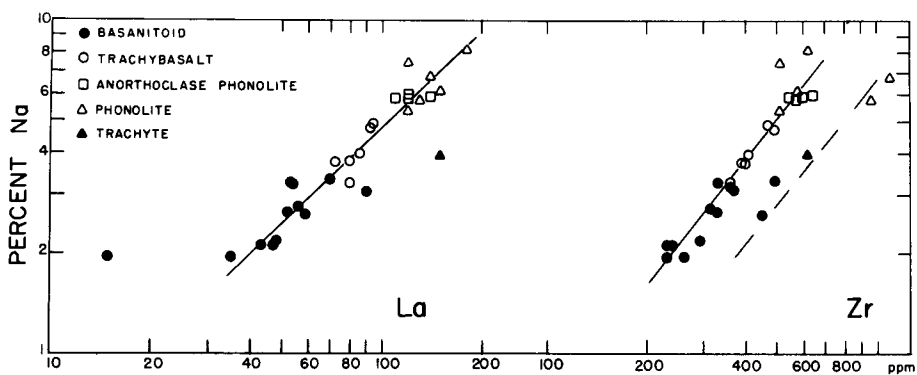
FIG. 7.—Variations of La and Zr with Na
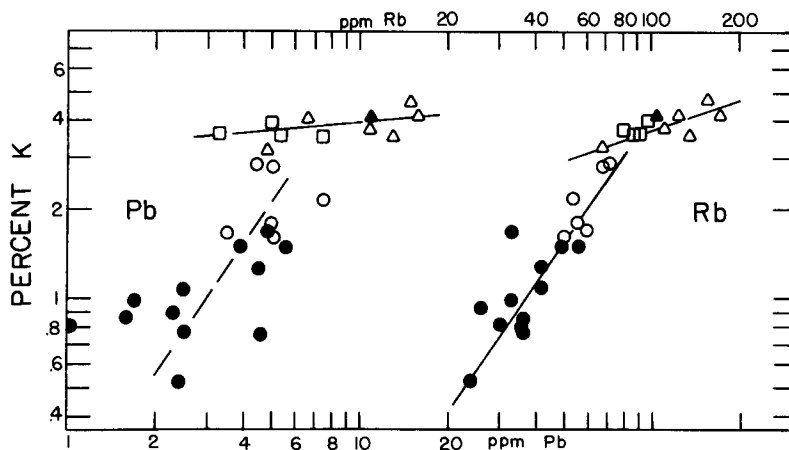
FIG. 8.—Variations of Pb and Rb with K
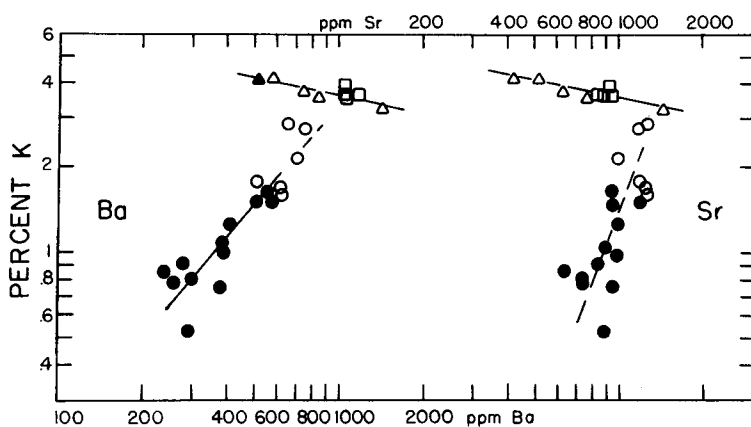
FIG. 9.—Variations of Ba and Sr with K

TABLE 10

AVERAGE CHEMICAL COMPOSITION OF ROCK TYPES

	30	31	32	33	34
SiO_2	43.26	44.86	49.95	55.78	56.15
Al_2O_3	13.36	16.83	18.50	19.28	20.47
TiO_2	3.31	3.49	2.31	1.09	0.64
Fe_2O_3	3.67	7.23	2.88	1.86	3.10
FeO	8.44	4.81	5.65	4.02	1.58
MnO	0.20	0.23	0.20	0.21	0.19
MgO	10.62	4.10	2.57	1.21	0.71
SrO	0.11	0.15	0.14	0.11	0.07
CaO	11.01	9.49	6.93	3.30	2.55
BaO	0.04	0.07	0.08	0.12	0.08
Na_2O	3.49	4.93	5.98	7.91	8.85
K_2O	1.25	2.05	3.11	4.38	4.68
P_2O_5	0.70	1.49	0.97	0.46	0.18
H_2O^+	0.28	0.20	0.39	0.19	0.31
H_2O^-	0.15	0.07	0.11	0.09	0.16
CO_2	0.10	0.02	0.04	0.03	0.03
Total	100.00	100.02	99.81	100.04	99.75

NOTE.—*30*, Average basanitoid (table 1, nos. 1–12); *31*, average low-silica trachybasalt (table 2, nos. 13–15); *32*, average high-silica trachybasalt (table 2, nos. 16–18); *33*, average anorthoclase phonolite (table 3, nos. 19–22); and *34*, average phonolite (table 4, nos. 23–28).

and trachybasalts, but the trends are reversed in the phonolites, and Ba and Sr decline with increasing K.

DISCUSSION

Magmatic differentiation.—The variations of major, minor, and trace elements support a differentiation model controlled by fractional crystallization from alkali olivine basalt → trachybasalt → phonolite. The basanitoids contain phenocrysts of olivine, clinopyroxene, and opaque minerals, and the crystallization of these phases governed the early differentiation trend. Although there may have been original differences in the basanitoid parental magmas, the scatter in the points for MgO (fig. 4) probably is largely the result of settling of olivine. The MgO content of the basanitoids ranges from 7.8% to 13% with a corresponding range in Ni content from less than 150 to 300 ppm (table 5).

The differentiation trends may be seen in the variations of major and trace constituents in figures 10 and 11 in which averages for the principal rock types are plotted against K_2O. The diagrams show the close relationship between the low silica trachybasalts and the basanitoids. Removal of olivine, clinopyroxene, and opaque oxides enriched the liquid in Rb, Zr, Sr, Ba, and others (fig. 10); V, Co, and Cu were depleted (fig. 11); P_2O_5 was notably enriched, and to a lesser extent, also TiO_2 and Al_2O_3; Rb, La, and Zr (fig. 10) were enriched progressively with a sharp increase in the phonolites. Sr attained maximum concentration in the low-silica trachybasalts, and was strongly controlled by crystallization of plagioclase. Ba was progressively enriched from the basanitoids through the trachybasalts and anorthoclase phonolites in which it is concentrated in the anorthoclase (Mountain 1925; Boudette and Ford 1966; Treves 1967).

Analyses of other mineral phases are in progress, and these will permit a more quantitative treatment of the magmatic differentiation processes. The preliminary chemical results, together with the major and trace-element analyses of this paper, indicate that the crystalizatlion of olivine,
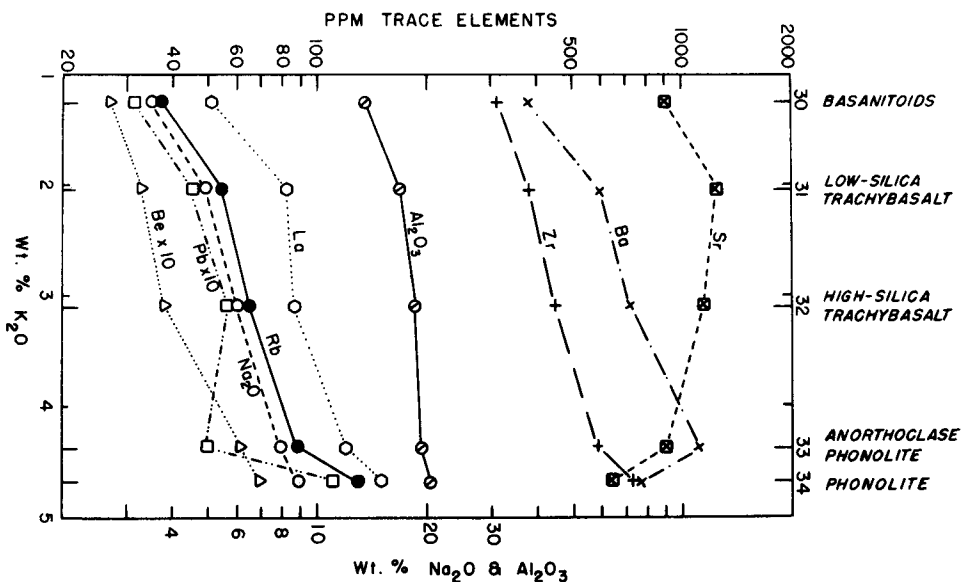
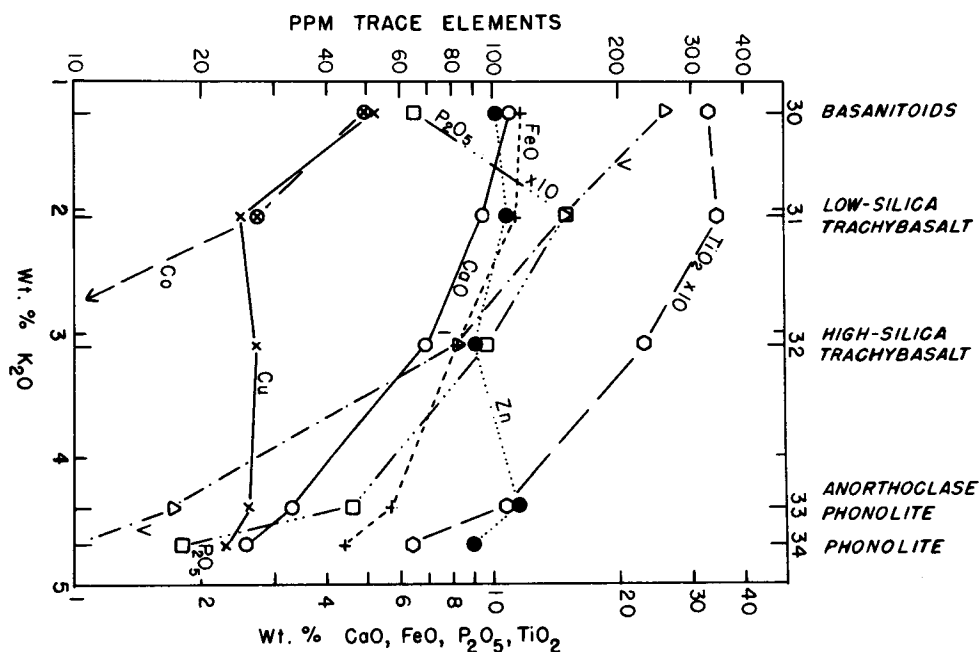Fig. 10.—Variations of Na₂O, Al₂O₃, Sr, Ba, Zr, La, Rb, Pb, and 'Be with K₂O in principal rock types.

Fig. 11.—Variations of CaO, FeO, P₂O₅, TiO₂, V, Zn, Cu, and Co with K₂O in principal rock types.

clinopyroxene, and opaque minerals clearly controlled the early stages of differentiation, giving way to clinopyroxene, apatite, and opaques, with plagioclase, kaersutite, and anorthoclase becoming later phases.

Parental magma.—Gast (1968) demonstrated that trace elements—particularly the large cations Rb, Ba, and Sr, and the rare earths—are useful in formulating a model for the derivation of basaltic liquids by partial melting of peridotitic mantle. A large degree (20%–30%) of partial melting would produce a tholeiitic magma; a small degree (3%–7%) would yield alkali-rich basaltic liquid. The origin of alkali-basalt magma is more fully discussed by Kay (Kay and Gast 1973) who suggests that nepheline normative alkali basalts, similar in composition to the basanitoids of the Ross Island vicinity, may be derived by a small degree (1%–2%) of partial melting of hydrous garnet peridotite near the top of the asthenosphere.

The $^{87}Sr/^{86}Sr$ data support the derivation of the basanitoid magma from mantle sources. Halpern (1969) determined $^{87}Sr/^{86}Sr$ ratios for an ultramafic nodule and the host basalt from the McMurdo area and for two ultramafic nodules from Mt. Perkins in the Ford Ranges and concluded from the ratios of 0.7030 to 0.7034 that the nodules and basalt probably are cogenetic. Jones and Walker (1972) reported a large number of Sr isotope ratios for volcanic rocks from Southern Victoria Land. The samples include representatives of the principal rock types from the Ross Island vicinity, and all have $^{87}Sr/^{86}Sr$ ratios in the range from 0.7020 to 0.7048. The Sr isotope ratios support the magmatic differentiation explanation for the rock series and are in agreement with data for alkalic rocks in other regions (Hedge 1966; Peterman and Hedge 1971).

Petrologic comparisons.—As would be expected, there are marked similarities between the volcanic rocks of the Ross Island vicinity and those of the Hallett province (Hamilton 1972). The flows in the Hallett region show the Ross Island trend: alkalic olivine basalt → trachybasalt → phonolite, but as Hamilton (1972, p. C59) indicates, there probably is a second rock series with the sequence: olivine basalt → latite → trachyte → quartz trachyte. If the composition of the trachyte from Mt. Cis in the Ross Island area has not been strongly altered by contamination, it may well belong to this second differentiation series. The analyzed samples from the Ross Island vicinity are less altered, with low ferric/ferrous iron ratios, and with little or no normative hematite compared with the Hallett volcanics. Hamilton (1972) attributes the oxidation to steam generated during eruptions beneath ice sheets in the Hallett region; whereas the eruptions in the Ross Island vicinity in large part were subaerial.

The basanitoids and derivatives in the Ross Island region are chemically similar to volcanic rocks in other areas, such as the Comores (Strong 1972a, 1972b,; Flower 1973; Thompson and Flower 1971). In an AMF diagram (fig. 12), the analyses from Ross Island plot close to the curve for the Hawaiian alkalic trend (Macdonald and Katsura 1964). The data points are largely bracketed by the Tristan (Baker et al. 1964) and Hebridean (Tilley and Muir 1962) or Icelandic (Carmichael 1964) curves.

Alkali basalts are related to rift zones on the continents and not to the major oceanic rifts or rises where tholeiitic or low-potassium basaltic magma is generated in large volumes. The association of alkali basalt with rift zones has been discussed in a number of papers, as for example, the East African Rift zone in Ethiopia (Mohr 1971), the Rio Grande depression (Lipman 1969), and the Balcones province, Texas (Spencer 1969). The parallelism of the belt of volcanic centers with the trend of the Transantarctic Mountains (fig. 1) suggests a regional structural control. As
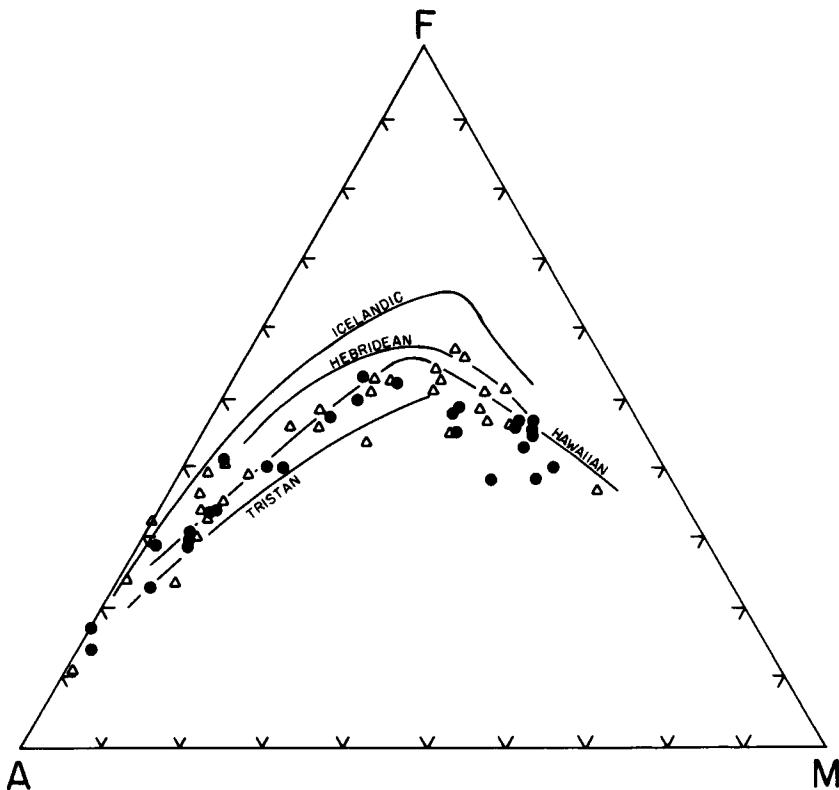
FIG. 12.—AMF diagram (wt%); symbols for Antarctica rocks are same as in figure 5. Reference trends are Icelandic Thingmuli series (Carmichael 1964); Hebridean (Tilley and Muir 1962); Hawaiian alkalic trend (Macdonald and Katsura 1964); and Tristan (Baker et al. 1964).

in many other parts of the world, the alkalic rocks of the Antarctic belt probably are related to tensional forces that may have permitted rapid ascent of the magma.

APPENDIX

SAMPLE LOCATION AND DESCRIPTION

Numbers refer to figures 1, 2, and 3; field numbers in parentheses. All samples are fine-grained and gray to black.

BASANITOIDS

1, (12167) Younger flow, Brown Peninsula (fig. 3). Olivine phenocrysts (2 mm), 16%; groundmass: clinopyroxene, plagioclase, opaques, olivine, nepheline, and apatite. Minor carbonate and alteration of olivine.

2, (2467) Younger, unglaciated sequence on Mt. Hayward, White Island (fig. 3). Phenocrysts: olivine, 7%; clinopyroxene, 0.1%.

3, (15670) Younger sequence, summit of Mt. Morning (fig. 3). Large yellowish olivine, 23%; black vitreous clinopyroxene, 13%.

4, (4267) Older sequence north of Mt. Heine, White Island (fig. 3). Green olivine (3 mm), 28% black clinopyroxene, 6%.

5, (267) Small vent on the south side of Taylor Valley at western edge of Sollas Glacier (fig. 1). Olivine (1 mm), 9%; clinopyroxene, 6%. Samples from small vents in this area have been dated at 2.7 m.y. (Armstrong et al. 1968).

6, (10567) Brandau Vent, Royal Society Range (fig. 3). Described by McIver and Gevers (1970, p. 76). Green olivine, 12%; black clinopyroxene, 13%.

7, (15367) Younger sequence on Cape Crozier, Ross Island (fig. 2). Green olivine, 14%; black clinopyroxene, 7%; black kaersutite, 4%; subhedral plagioclase ($\sim An_{50}$), 3%.

8, (15765) Older sequence on Cape Armitage, Ross Island (fig. 2). Large green olivine, 24%; clinopyroxene, 8%; opaque, 4.5%.

9, (11667) Core of a pillow, older flow on Brown Peninsula (fig. 3). Yellowish olivine, 6%; black clinopyroxene, 7%; kaersutite, 7%.

10, (567) Older sequence, Cape Crozier, Ross Island (fig. 2). Olivine, 13%; clinopyroxene, 14%; kaersutite, 1%.

11, (16170) Summit of Mt. Bird, Ross Island (fig. 2). Yellowish-green olivine (3 mm), 8%; clinopyroxene (2 mm), 3% in glassy matrix.

12, (7367) Younger sequence, Mt. Melania, Black Island (fig. 3). Small yellowish-green olivine, 2%; clinopyroxene, 3%.

TRACHYBASALTS

13, (14870) Brownish-black, fine-grained; Mt. Terra Nova, Ross Island (fig. 2). Phenocrysts of subhedral plagioclase ($\sim An_{49}$), 22%; small olivine, 1.5%. Groundmass: clinopyroxene, opaques, apatite, and glass.

14, (14770) Same locality as No. 13. Hornblende, 10%; plagioclase ($\sim An_{52}$), 4%; clinopyroxene, 3%; opaque, 2.5%. Groundmass: clinopyroxene, plagioclase, opaque, and glass.

15, (12765) Basalt Hill, southeast of Cape Royds, Ross Island (fig. 2). Basalt of Smith (1954, p. 99). Plagioclase ($\sim An_{50}$), 37%; clinopyroxene, 8%; olivine, 2%. Groundmass: clinopyroxene, plagioclase, opaque, and apatite.

16, (7467) Near Mt. Melania, Black Island (fig. 3). Plagioclase ($\sim An_{56}$), 38%; opaque, 6%; olivine, 3%. Groundmass largely glass

with plagioclase, opaque, olivine, clinopyroxene, and apatite.

17, (14167) Miers Valley (fig. 3). Large subhedral phenocrysts of plagioclase ($\sim An_{53}$), 27%; clinopyroxene, 5%; opaque, 3%; olivine, 2%.

18, (201) Tryggve Point (fig. 2). Large, subhedral zoned plagioclase phenocrysts ($\sim An_{37}$), 33%; olivine, 7%; clinopyroxene, 2%; opaque, minor. Groundmass: plagioclase, clinopyroxene, olivine, opaques.

ANORTHOCLASE PHONOLITES

19, (14467) Cape Evans, Ross Island (fig. 2); kenyte of Smith (1954). Phenocrysts: anorthoclase, 42%; clinopyroxene, 1.6%. Groundmass: anorthoclase, 63%; clinopyroxene, 37%; opaque, apatite, and nepheline.

20, (13770) Summit of Mt. Erebus, Ross Island (fig. 2). Anorthoclase, 31%; clinopyroxene, 1%. Groundmass largely glass with some clinopyroxene, apatite, nepheline, and opaques.

21, (15267) Youngest flow of anorthoclase phonolite at Cape Royds, Ross Island (fig. 2); leucite kenyte of Prior (1907); anorthoclase trachyte of Boudette and Ford (1966). Phenocrysts: anorthoclase, 38%; clinopyroxene, 1%; olivine 0.4%.

22, (15167) From the same flow as no. 21. Phenocrysts: anorthoclase, 30%; clinopyroxene, 1%; olivine, 0.5%. Groundmass largely glass.

HORNBLENDE AND PYROXENE PHONOLITES

23, (15067) Flow within the older sequence near the summit of Mt. Discovery (fig. 3). Phenocrysts: large plagioclase ($\sim An_{26}$), 31%; opaques, 2%; clinopyroxene, 1%; olivine, trace. Groundmass: clinopyroxene, plagioclase, minor apatite and opaques.

24, (16070) Mt. Bird, Ross Island (fig. 2). Phenocrysts: anorthoclase, 20%; plagioclase ($\sim An_{28}$), 12%; clinopyroxene, 4%; kaersutite, 2%. Groundmass: anorthoclase, clinopyroxene, and opaques.

25, (15965) Observation Hill, Ross Island (fig. 2); hornblende trachyte of Prior (1907). Phenocrysts: anorthoclase, 32%; hornblende, 10%; plagioclase, 3%; clinopyroxene, 1%,

26, (5867) Light olive-gray vitric phonolite from Mt. Aurora, Black Island (fig. 3). Partially devitrified, somewhat vesicular glass with finely disseminated opaques and a few microlites of plagioclase.

27, (8567) Glomeroporphyry from Minna Bluff (fig. 3). Anorthoclase phenocrysts, 4%. Groundmass largely anorthoclase, clinopyroxene, and trace of opaques.

28, (1167) Gray, fine-grained, vesicular rock from Post Office Hill, Cape Crozier, Ross Island (fig. 2). Phenocrysts: anorthoclase, 17%; reddish-brown hornblende, 7%.

TRACHYTE

29, (13867) Fine-grained, olive-gray rock from Mt. Cis, near Cape Royds, Ross Island (fig. 2); trachyphonolite of Jensen (1916), phonolitic trachyte of Smith (1954). Clinopyroxene phenocrysts, about 1%. Groundmass: anorthoclase, clinopyroxene, opaques, apatite, and carbonate.

REFERENCES CITED

ARMSTRONG, R. L.; HAMILTON, W.; and DENTON, G. H., 1968, Glaciation in Taylor Valley, Antarctica, older than 2.7 million years: Science, v. 159, p. 187–189.

BAKER, P. E.; GASS, I. G.; HARRIS, P. G.; and LeMAITRE, R. W., 1964, The volcanological report of the Royal Society expedition to Tristan da Cunha, 1962: Royal Soc. (London) Philos. Trans., ser. A, no. 256, p. 439–578.

BOUDETTE, E. L., and FORD, A. B., 1966, Physical properties of anorthoclase from Antarctica: Am. Mineralogist, v. 51, p. 1374–1387.

CARMICHAEL, I. S. E., 1964, The petrology of Thingmuli, a Tertiary volcano in eastern Iceland: Jour. Petrology, v. 5, p. 409–434.

COLE, J. W., and EWART, A., 1968, Contributions to the volcanic geology of the Black Island, Brown Peninsula, and Cape Bird areas, McMurdo Sound, Antarctica: New Zealand Jour. Geology and Geophysics, v. 11, p. 793–828.

COMPSTON, W.; McDOUGALL, I.; and HEIER, K. S., 1968, Geochemical comparison of the Mesozoic basaltic rocks of Antarctica, South Africa, South America and Tasmania: Geochim. et Cosmochim. Acta, v. 32, p. 129–149.

FLOWER, M. F. J., 1973, Evolution of basaltic and differentiated lavas from Anjouan, Comores Archipelago: Contr. Mineralogy and Petrology, v. 38, p. 237–260.

FORBES, R. B., 1963, Ultrabasic inclusions from the basalts of the Hut Point area, Ross Island, Antarctica: Bull. volcanol., v. 26, p. 13–21.

———, and KUNO, H., 1965, The regional petrology of peridotite inclusions and basaltic host rocks: I. U. G. S. Upper Mantle Symposium, New Delhi 1964, Copenhagen, p. 161–180.

GAST, P. W., 1968, Trace element fractionation and the origin of tholeiite and alkaline magma types: Geochim. et Cosmochim. Acta, v. 32, p. 1057–1086.

HALPERN, M., 1969, $^{87}Sr/^{86}Sr$ ratios of ultramafic nodules and host basalt from the McMurdo area and Ford Ranges, Antarctica: Antarctic Jour. U.S., v. 4, p. 206.

HAMILTON, W., 1972, The Hallett volcanic province, Antarctica: U.S. Geol. Survey Prof. Paper 456-C, 62 p.

HEDGE, C., 1966, Variations in radiogenic strontium found in volcanic rocks: Jour. Geophys. Research, v. 71, p. 1214–1217.

INGAMELLS, C. O., and SUHR, N. H., 1963, Chemical and spectrochemical analysis of standard silicate samples: Geochim. et Cosmochim. Acta, v. 27, p. 897–910.

JENSEN, H. I., 1916, Report on the petrology of the alkaline rocks of Mount Erebus, Antarctica: British Antarctic Expedition 1907–9: Rept. Sci. Inv. Geology, v. 2, p. 93–128.

JONES, L. M., and Walker, R. L., 1972, Geochemistry of the McMurdo volcanics, Victoria Land: Part 1, Strontium isotope composition: Antarctic Jour. U.S., v. 7, p. 142–144.

KAY, R. W., and GAST, P. W., 1973, The rare earth content and origin of alkali-rich basalts: Jour. Geology, v. 81, p. 653–682.

LIPMAN, P. W., 1969, Alkalic and tholeiitic basaltic volcanism related to the Rio Grande depression, southern Colorado and northern New Mexico: Geol. Soc. America Bull., v. 80, p. 1343–1354.

MACDONALD, G. A., and KATSURA, T., 1964, Chemical composition of Hawaiian lavas: Jour. Petrology, v. 1, p. 172–177.

McDOUGALL, I., 1963, Potassium-argon age measurements on dolerites from Antarctica and South Africa: Jour. Geophys. Research, v. 68, p. 1535–1545.

McIVER, J. R., and Gevers, T. W., 1970, Volcanic vents below the Royal Society Range, Central Victoria Land, Antarctica: Geol. Soc. South Africa, v. 73, p. 65–68.

MEDLIN, J. H.; SUHR, N. H.; and BODKIN, J. B., 1970, Determination of rubidium in silicate materials by atomic absorption spectrophotometry: Chem. Geology, v. 6, p. 143–148.

MOHR, P. A., 1971, Ethiopian rift and plateau: some volcanic petrochemical differences: Jour. Geophys. Research, v. 76. p. 1967–1985.

MOUNTAIN, E. D., 1925, Potash-oligoclase from Mt. Erebus, Antarctica, and anorthoclase from Mt. Kenya, East Africa: Mineralog. Mag., v. 20, p. 331–345.

PETERMAN, Z. E., and HEDGE, C. E., 1971, Related strontium isotopic and chemical variations in oceanic basalts: Geol. Soc. America Bull., v. 82, p. 493–500.

PRIOR, G. T., 1902, Report on the rock-specimens collected by the "Southern Cross" Antarctic Expedition: Brit. Mus. (Nat. Hist.), p. 321–332.

————, 1907, Report on rock specimens collected during the "Discovery" Antarctica Expedition, 1901–1904: Brit. Mus. Rep. 1 (Geology), p. 101–123.

SMITH, W. C., 1954, The volcanic rocks of the Ross Archipelago: British Antarctic "Terra Nova" Expedition, 1910: Nat. Hist. Rept. Geology, v. 2, p. 1–107.

SPENCER, A. B., 1969, Alkalic igneous rocks of the Balcones province, Texas: Jour. Petrology, v. 10, p. 272–306.

STRONG, D. F., 1972a, The petrology of the lavas of Grande Comore: Jour. Petrology, v. 13, p. 181–217.

————, 1972b, Petrology of the Island of Moheli, Western Indian Ocean: Geol. Soc. America Bull., v. 83, 389–405.

THOMPSON, J. A., 1916, Report on the inclusions of the volcanic rocks of the Ross Archipelago, British Antarctic Expedition 1907–1909, Geol. Rept. 2, p. 129–148.

THOMPSON, R. N., and FLOWER, M. F. J., 1971, One-atmosphere melting and crystalline relations of lava from Anjouan, Comores Archipelago, Western Indian Ocean: Earth and Planetary Sci. Letters, v. 12, p. 97–107.

TILLEY, C. E., and MUIR, I. D., 1962, The Hebridean plateau magma type: Edinburgh Geol. Soc., Trans., v. 19, p. 208–215.

TREVES, S. B., 1967, Volcanic rocks from the Ross Island, Marguerite Bay, and Mount Weaver areas, Antarctica: Japanese Antarctic Research Expedition (JARE) Scientific Reports, v. 1, p. 136–149.